Effect of Mg^{2+} Doping on the Structural, Thermal, and Electrochemical Properties of $LiNi_{0.8}Co_{0.16}Mg_{0.04}O_2$

A. D'Epifanio,*,‡ F. Croce,|| F. Ronci,§ V. Rossi Albertini,§ E. Traversa,‡ and B. Scrosati†

Dipartimento di Chimica, Università di Roma "La Sapienza", 00185, Italy, Dipartimento di Scienze e Tecnologie Chimiche, Università di Roma "Tor Vergata", 00100, Italy, Istituto di Struttura della Materia, Area di ricerca di Tor Vergata del CNR, 00133 Roma, Italy, and Dipartimento di Scienze del Farmaco, Università "G. D'Annunzio", 66013 Chieti, Italy

Received April 20, 2004

$LiNi_{0.8}Co_{0.16}Mg_{0.04}O_2$ layered oxide samples were synthesized by a chemical route that led to a crystalline phase at a relatively low temperature and allowed the control of the homogeneity and the microstructural properties of the final compounds. The structural properties of the synthesized sample were investigated by performing XRD Rietveld refinement. The role of the doping metal (Mg^{2+}) on the electrochemical characteristics of this layered oxide was investigated via its use as cathode material in a lithium cell and observation of its structural evolution upon cycling by in-situ energy dispersive X-ray diffraction (EDXD). The thermal stability of the delithiated $Li_xNi_{0.8}Co_{0.16}Mg_{0.04}O_2$ cathodes was evaluated using differential scanning calorimetry (DSC). The results demonstrate that the Mg^{2+} doping greatly reduces the unit cell volume change during cycling, because of a very limited variation of the *c* lattice parameter. This improved structural retention also reflects an improvement of the stability of the doped cathode in its fully charged state.

Introduction

Intense research is worldwide devoted to the synthesis and characterization of positive electrode materials for lithium ion batteries.[1] Most of the efforts are concentrated on two-dimensional layer-structured, alkali transition metal oxides because $LiCoO_2$ is still the cathode of choice for the majority of the commercial rechargeable Li-ion batteries.[2] The goal is to develop and optimize cathodic materials, different from $LiCoO_2$, that may operate as cheaper substitutes. In this respect, an interesting candidate is $LiNiO_2$, a compound that has the same crystal structure as $LiCoO_2$, but a lower cost associated with potentially appealing electrochemical performances. Unfortunately, the practical use of this nickel oxide compound is affected by a poor structural stability upon cycling. This generates safety concerns about exothermic decomposition phenomena of $LiNiO_2$ in its charged state, which is associated with the instability of nickel in the high oxidation state.[3−5]

Attempts to stabilize the $LiNiO_2$ structure have been directed to metal substitution for nickel. Promising results have been obtained with $LiNi_yCo_{1-y}O_2$ mixed compounds,[6,7] where the addition of Co stabilizes the desired two-dimensional layered structure,[8] this substantially improving the cycle life and the rate of the electrodes. However, these performances are not accompanied by improvements in safety because also $Li_xNi_yCo_{1-y}O_2$ compounds are unstable in their charged state ($x \simeq 0.5$).[3] Under this condition, thermal runaway of the cell may occur with release of oxygen into the electrolyte, which in turn may lead to violent reactions.[4,5]

It has been suggested[9,10] that doping with extra M metals (M = Al, Mg, ...) may consistently improve the thermal stability of the electrode. However, the correlation between this enhancement in stability and structure retention of the doped $LiNi_{0.8}Co_{0.16}Mg_{0.04}O_2$ electrode materials has not been so far fully ascertained. In a previous work,[11] we have demonstrated this correlation by monitoring in-situ the structural evolution of $LiNi_yCo_{1-y-z}Al_zO_2$ by using an in-house recently developed method, which is based on the energy dispersive X-ray diffraction (EDXD) technique.[12] In this work, we apply the same technique to the $LiNi_{0.8}Co_{0.16}Mg_{0.04}O_2$ case.

* To whom correspondence should be addressed. E-mail: alessandra.d.epifanio@uniroma2.it.
† Università di Roma "La Sapienza".
‡ Università di Roma "Tor Vergata".
§ Istituto di Struttura della Materia.
|| Università "G. D'Annunzio".

(1) Scrosati, B. *Electrochim. Acta* **2000**, *45*, 2461.
(2) Vincent, C. A. *Solid State Ionics* **2000**, *134*, 159.
(3) Dahn, J. R.; Fuller, E. W.; Obrovac, M.; von Sacken, U. *Solid State Ionics* **1994**, *69*, 265.
(4) Gao, Y.; Yakovleva, M. V.; Ebner, W. B. *Electrochem. Solid-State Lett.* **1998**, *1*, 117.
(5) Cho, J.; Jung, H.; Park, Y.; Kim, G.; Lim, H. S. *J. Electrochem. Soc.* **2000**, *147*, 15.
(6) Li, W.; Currie, J. C. *J. Electrochem. Soc.* **1997**, *144*, 2773.
(7) Croce, F.; Deptula, A.; Lada, W.; Marassi, R.; Olczac, T.; Ronci, F. *Ionics* **1997**, *3*, 390.
(8) Zhecheva, E.; Stoyanova, R. *Solid State Ionics* **1993**, *66*, 143.
(9) Delmas, C.; Saadoune, I. *Solid State Ionics* **1992**, *370*, 53.
(10) Reimers, J. N.; Rossen, E.; Jones, C. D.; Dahn, J. R. *Solid State Ionics* **1992**, *311*, 53.
(11) D'Epifanio, A.; Croce, F.; Ronci, F.; Rossi Albertini, V.; Traversa, E.; Scrosati, B. *Phys. Chem. Chem. Phys.* **2001**, *3*, 4399.
(12) Ronci, F.; Scrosati, B.; Rossi Albertini, V.; Perfetti, P. *Electrochem. Solid-State Lett.* **2000**, *3*, 174.

10.1021/cm040130x CCC: $27.50
Published on Web 08/05/2004

Experimental Section

A chemical route based on an optimized polymeric precursor decomposition process[13,14] was used to prepare $LiNi_{0.8}Co_{0.16}Mg_{0.04}O_2$ oxide. Details of this synthesis have already been reported elsewhere for $LiNi_{0.8}Co_{0.16}Al_{0.04}O_2$.[11] $LiCH_3COO\cdot 2(H_2O)$ (Aldrich 99%), $Ni(CH_3COO)_2\cdot 4(H_2O)$ (Aldrich 98%), $Co(CH_3COO)_2\cdot 4(H_2O)$ (Aldrich 98%), $Mg(CH_3COO)_2\cdot 4(H_2O)$ (Aldrich 99%), and citric acid, in stoichiometric amounts, were dissolved in ethylene glycol. The solution obtained was heated at 120 °C to form a gel, the transparency of which was an indication of the reached homogeneity of the system. Subsequently, the gel was dried at 120−140 °C for about 48 h and then calcined at 750 °C in air for 15 h to obtain the crystalline phase of the $LiNi_{0.8}Co_{0.16}Mg_{0.04}O_2$ oxide.

To investigate the evolution of the thermal process occurring during heat treatment of the sol complex (i.e., the $LiNi_{0.8}Co_{0.16}Mg_{0.04}$ complex), simultaneous thermogravimetric and differential thermal analyses (TGA/DTA) were performed, using a thermoanalyzer (STA 409, Netzsch) in air flow (80 $cm^3\ min^{-1}$) at a heating rate of 10 °C min^{-1} between 25 and 1200 °C. The chemical composition of the final powder was determined by ICP-AES (inductively coupled plasma-atomic emission spectroscopy) analysis after dissolution of the powder in HCl. X-ray diffraction (XRD) analysis of the samples was carried out after thermal treatment by means of a Philips x'Pert MPD powder diffractometer equipped with a Cu Kα radiation source and graphite monochromator. The Rietveld refinement was performed using the Fullprof[15] software. The morphology of the powder was observed using a scanning electron microscope (SEM).

The cathodic membranes were prepared by mixing the active material with PVdF (poly(vinylidenefluoride) Solvay Solef 6020) as a binder with a Super P (MMM Belgium) weight ratio of 82:10:8 in NMP (1-methyl-2-pyrrolidone) to form a slurry. The slurry was cast on an Al foil and dried at about 120 °C under vacuum for 24 h. The electrochemical cells were assembled by combining the cathodic membranes with a glass fiber separator (Whatman GF/A) soaked with an EC:DEC (1:1) $LiClO_4$ 1 M liquid electrolyte and with a high-purity lithium foil (Cyprus Foote) anode. The real-time structural evolution of the $LiNi_{0.8}Co_{0.16}Mg_{0.04}O_2$ cathodic material was observed in-situ by energy dispersive X-ray diffraction, EDXD. The advantages of this technique in comparison with the conventional (angular dispersive) laboratory X-ray powder diffraction have been outlined in previous works.[12,16−19] They can be summarized as follows.

(1) The first advantage is the use of high-energy (up to 60 keV) polychromatic radiation as the primary beam. The integrated intensity of this beam, in typical operating conditions, is about an order of magnitude higher than that of the monochromatic radiation (generally the 8.04 keV Cu Ka fluorescence line) used in the angular dispersive mode, so that the acquisition time is proportionally reduced. Furthermore, the higher energy of the primary beam results in a lower X-ray absorption, which is the main cause of signal reduction in this kind of in-situ measurement.

As a consequence of these two facts, batteries having standard design can be utilized, preventing problems coming from the unusual geometry and extreme thinness required when lower energy X-ray beams are utilized.

(2) The experimental apparatus is fixed, no movement being required to perform the reciprocal space scan. Indeed, the scan is carried out electronically, instead of mechanically, and, for this reason, no misalignments or change in the diffracting volume, which would compromise the results, may occur. Therefore, the diffraction patterns can be collected in a fast and reliable way, and the lattice parameters versus the intercalation degree curves are sampled densely, so that even the minimal details can be detected. In fact, the curves of Figure 5 have the aspect of continuous lines, rather than of a collection of isolated points.

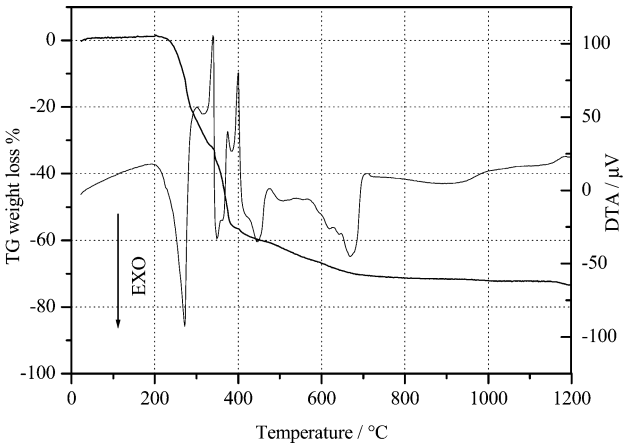

Figure 1. TG/DTA analyses of gel precursors in the synthesis of the $LiNi_{0.80}Co_{0.16}Mg_{0.04}O_2$ sample.

To run the EDXD in-situ test, the cycling current was fixed at $I = 41.1\ \mu A$ both in charge and in discharge. The cathodic and anodic limits were fixed at 3.1 V and from 4.5 to 5.0 V, respectively. The latter was raised by 0.1 V per cycle to observe the effect of the progressive increase of the delithiation degree on the $LiNi_{0.8}Co_{0.16}Mg_{0.04}O_2$ lattice structure. The diffraction patterns were collected sequentially at a constant acquisition time of 20 min (corresponding to a $\Delta x = 0.05$) and, to obtain the values of the *a* and *c* lattice parameters, were refined using a home-developed software based on the Levenberg−Marquardt NLLS algorithm.

The stability of the cathode was compared to that of a commercial $Li_xNi_{0.8}Co_{0.2}O_2$ sample via differential scanning calorimetry (DSC).

For this test, the two cathodes were cycled galvanostatically in lithium cells using a EC:DEC $LiPF_6$ electrolyte at a *C*/5 rate for two cycles, and then they were kept potentiostatically at 4.2 V until the current was less than *C*/20 to reach an amount of extracted lithium of about 0.5 equiv. After the cycling, the cells were opened in a drybox, and the cathode powders were separated from the Al-foil current collector and hermetically sealed in DSC sample pans.

The DSC experiments were run using an 821 Mettler Toledo calorimeter at a ramp rate of 5 °C min^{-1} and over a range extending from room temperature to 400 °C. Exothermic and endothermic reactions as a function of the temperature are plotted as positive and negative heat flow, respectively. Only the active materials were considered to calculate the specific heat, and the curves were normalized to weight.

Results and Discussion

The optimal heat-treatment conditions for the synthesis of the $LiNi_{0.80}Co_{0.16}Mg_{0.04}O_2$ samples were determined by thermal analysis. Figure 1 shows the TGA/DTA traces of the precursor (Li−Ni−Co−Mg−citric acid−glycol). The total weight loss was observed to be about 70% and terminated at about 700 °C. The main weight loss (60%) appeared in a temperature range between 250 and 400 °C. In this range, the weight loss was associated with several exothermic and endothermic peaks in the DTA curve that are due to thermal decomposition mainly of the organic matrix. An exothermic peak centered at about 680 °C was attributed

(13) Pechini, M. P. U.S. Patent 3330697, 1967.
(14) Liu, M.; Wang, D. *J. Mater. Res.* **1995**, *10*, 3210.
(15) Rodriguez-Carvajal, J. Satellite Meeting on Powder Diffraction of the XV Congress of the IUCr, 1990, 127.
(16) Ronci, F.; Scrosati, B.; Rossi Albertini, V.; Perfetti, P. *J. Phys. Chem. B* **2001**, *105*, 754.
(17) Ronci, F.; Scrosati, B.; Rossi Albertini, V.; Perfetti, P. *Chem. Mater.* **2001**, *13*, 450.
(18) Robinson, K. M.; O'Grady, W. E. *Rev. Sci. Instrum.* **1993**, *64*, 1061.
(19) Giessen, B. C.; Gordon, G. E. *Science* **1968**, *159*, 973.

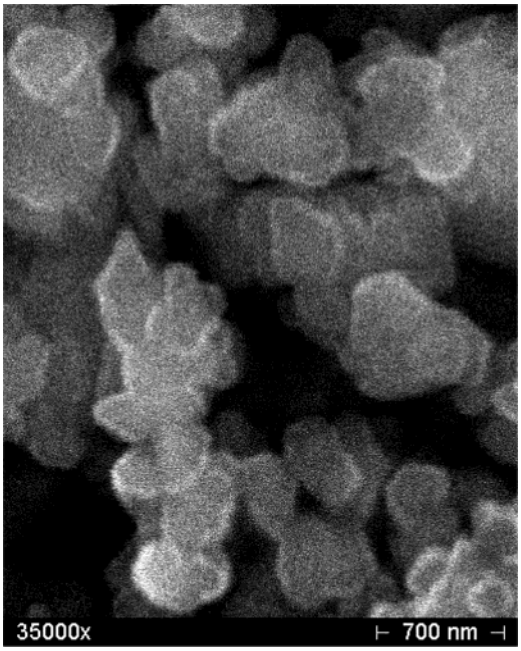

Figure 2. SEM picture of the $LiNi_{0.80}Co_{0.16}Mg_{0.04}O_2$ sample.

to the crystallization of the $LiNi_{0.80}Co_{0.16}Mg_{0.04}O_2$ hexagonal phase. At higher temperatures, no further reactions or weight losses were observed.

The chemical route here reported allows the formation of $LiNi_{0.80}Co_{0.16}M_{0.04}O_2$ at a lower temperature than the one required for the solid-state reaction synthesis.[20] This is an important aspect because high-temperature processes are generally to be avoided because they may lead to lithium deficiency in the final compound, due to the evaporation of lithium oxide.[3] In addition, high-temperature synthesis favors grain size growth.[6]

Figure 2 shows the SEM micrograph of the oxide formed by the decomposition at 750 °C of the precursor. Submicronic grains can be observed, but they result from a partial sintering of nanometric particles. Therefore, the synthesis allowed us to obtain powders with a very high porosity and a very high specific surface area.

The chemical composition of the powder, determined by ICP-AES, was found to be Li:Ni:Co:Mg = 0.99:0.80:0.16:0.04.

Figure 3 shows the XRD pattern, the Rietveld fit curve, and the difference plot of the $LiNi_{0.8}Co_{0.16}Mg_{0.04}O_2$ sample. A well-crystallized phase, isostructural with the parent compounds $LiNi_yCo_{1-y}O_2$, was observed. This result confirms that the addition of small amounts of dopant metals does not influence the basic $LiNi_yCo_{1-y}O_2$ structure ($R\bar{3}m$ space group).[11,21] On the basis of literature works on similar compounds,[24,25] we chose a model for refining the structure in which Mg and Ni ions were consented to occupy both the interslab (3b) and the slab

Table 1. Rietveld Refinement Results for the $LiNi_{0.80}Co_{0.16}Mg_{0.04}O_2$ Sample[a]

Space group						
$R\bar{3}m$						
Cell parameters						
a = 2.8671(5) Å						
c = 14.188(3) Å						
Ions parameters						
Ions	Site	Wyckoff position			Isotropic temperature	Occupancy
		x	y	z	factors B_{iso}(Å^2)	
Li^+	3b	0	0	0.5	0.8 (3)	0.942(8)
$Ni^{3+}{}_{3a}$	3a	0	0	0	0.646(4)	0.742(8)
$Ni^{2+}{}_{3b}$	3b	0	0	0.5	0.8(3)	0.058(8)
Co^{3+}	3a	0	0	0	0.646(4)	0.16
Mg^{2+}	3a	0	0	0	0.646(4)	0.04
O^{2-}	6c	0	0	0.2579(5)	1.20(8)	2.00
Profile parameters						
Profile function: pseudo-Voigt $pV = \eta L + (1-\eta)G$ where L=Lorentian, G=Gaussian and $\eta=\eta_0+X\cdot(2\Theta)$						
η_0 = 0.66(7) X = 0.003(2)						
U = 0.10(3) V = 0.024(2) W = 0.032(6)						
Constraints						
$n(Ni^{3+}{}_{3a}) + n(Ni^{2+}{}_{3b}) = 0.80$						
$n(Li^+{}_{3b}) + n(Ni^{2+}{}_{3b}) = 1$						
$B_{iso}(Ni^{3+}{}_{3a}) = B_{iso}(Co^{3+}) = B_{iso}(Mg^{2+})$						
$B_{iso}(Li^+) = B_{iso}(Ni^{2+}{}_{3b})$						
Reliability factors for points with Bragg contribution						
Rb = 4.27 Rwp = 12.5						

[a] The standard deviations were multiplied by the Scor parameter.[15]

(3a) sites, while Co ions were fixed in the 3a sites. Using this configuration, we found that Mg ions occupy only the 3a sites. As a consequence, we changed our model accordingly, as reported in Table 1, where the Rietveld refinement results are summarized. The cell parameters $a = b = 2.8659(6)$ Å and $c = 14.186(3)$ Å are in good agreement with literature data,[11,23,24] and the rather high value of the ratio $c/a = 4.95$ confirms the well-ordered layered character of the structure. The results on site occupancy showed that only a small amount of Ni ions were present in 3b sites, with Mg ions only in the 3a site, as mentioned above. Contrasting conclusions were drawn in the literature, for example, by Cho[25] and Pouillerie et al.[24] Our results confirm what was asserted by the former author.

The EDXD technique was used to describe the structural "breathing" of the sample lattice upon the lithium extraction−insertion process. Figure 4 shows the sequence of 427 diffraction patterns acquired during the cell cycling in the form of a 3D map as a function of the scattering parameter q (momentum transfer).

In this picture, the shift of the diffraction peaks during the lithium extraction−insertion process is clearly visible as the anodic limit is increased, particularly in the 4.2−4.6 V range (108, 110, and 113 peaks). The collected patterns were fitted to obtain the values

(20) Chang, C.-C.; Kumta, P. N. *J. Power Sources* **1998**, *75*, 44.
(21) Pouillerie, C.; Croguennec, L.; Biensan, Ph.; Willmann, P.; Delmas, C. *J. Electrochem. Soc.* **2000**, *147*, 2061.
(22) Caurant, D.; Baffier, N.; Garcia, B.; Pereira-Ramos, J. P. *Solid State Ionics* **1996**, *91*, 45.
(23) Rougier, A.; Saadoune, I.; Gravereau, P.; Willmann, P.; Delmas, C. *Solid State Ionics* **1996**, *90*, 83.
(24) Pouillerie, C.; Perton, F.; Biensan, Ph.; Peres, J. P.; Broussely, M.; Delmas, C. *J. Power Sources* **2001**, *96*, 293.
(25) Jang, Y. I.; Huang, B.; Wang, H.; Maskaly, G. R.; Ceder, G.; Sadoway, D. R.; Chiang, Y. M.; Liu, H.; Tamura, H. *J. Power Sources* **1999**, *81−82*, 589.

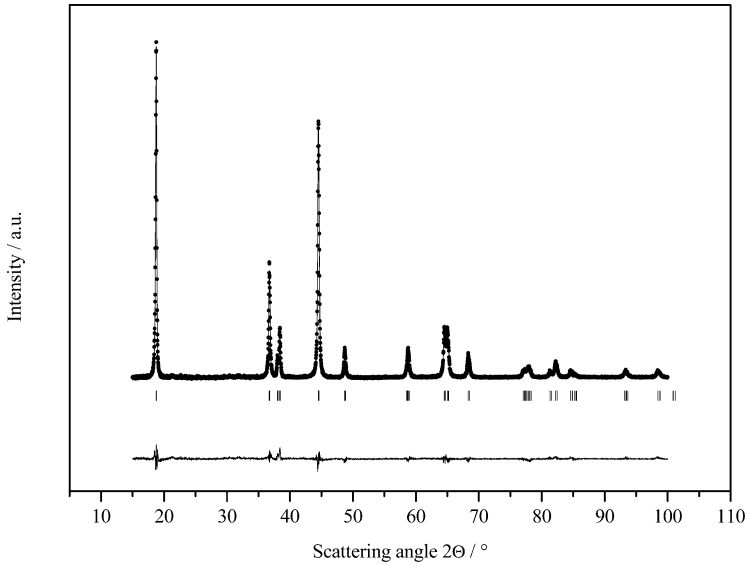

Figure 3. X-ray diffraction pattern of the $LiNi_{0.80}Co_{0.16}Mg_{0.04}O_2$ powder sample. The experimental (dotted) and fitted (line) curves are reported together with the difference curve.

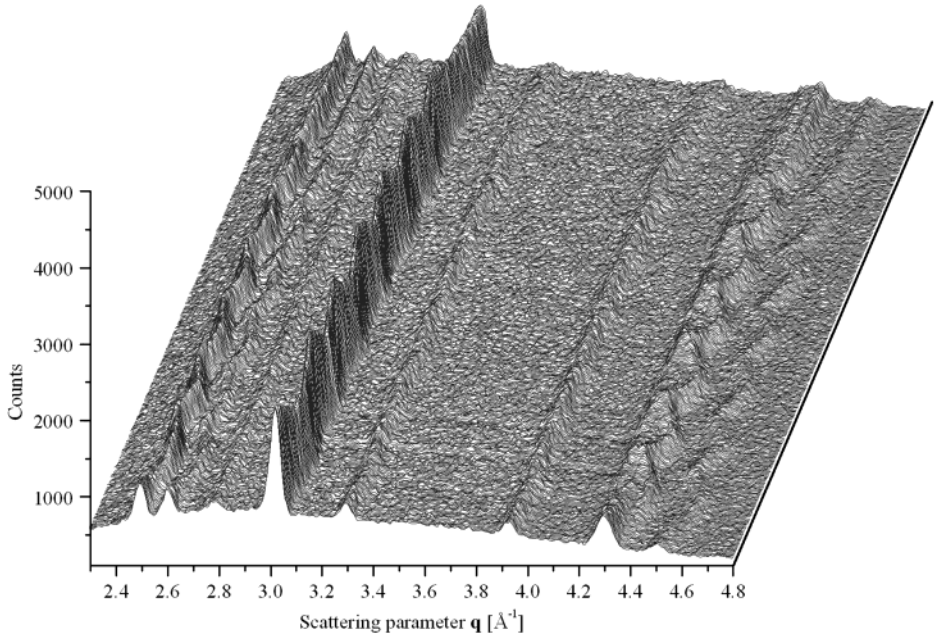

Figure 4. Sequence of 427 diffraction patterns of $LiNi_{0.80}Co_{0.16}Mg_{0.04}O_2$ collected upon cell cycling. In the first two cycles, the anodic limit was set at 4.5 V, while in the following cycles, it was increased by 0.1 V steps to 5.0 V.

of hexagonal lattice parameters ($a = b$, c). Figure 5 shows the evolution of the lattice parameters as a function of time, together with the calculated unit cell volume. In the same figure, the profiles of the electrochemical Li extraction−insertion process are also shown. As expected,[30,31] the a parameter decreases during the Li-extraction and increases during the Li-insertion. On the other hand, the c parameter shows a more complex trend, because, during the Li-extraction, it first increases until a certain threshold value and then it starts to decrease (and vice versa during the opposite Li-insertion cycle). The variation of the a parameter is found to be about 0.04 Å in all cycles except the first, so that $\Delta a/a < 1.5\%$. This result is in agreement with data reported in previous works on Al-doped ($LiNi_{1-x-y}Co_xAl_yO_2$) and undoped ($LiNi_{0.8}Co_{0.2}O_2$) oxides.[11,16] On the other hand, in the $LiNi_{0.80}Co_{0.16}Mg_{0.04}O_2$ case, the progressive increase of the anodic limit does not seem to influence the c parameter as was instead observed in both $LiNi_{0.8}Co_{0.2}O_2$ and $LiNi_{0.80}Co_{0.16}Al_{0.04}O_2$.[11,16]

Indeed, Figure 5 shows that the variation of c is limited to about 0.13 Å, corresponding to a $\Delta c/c < 1\%$. Such variation does not increase as the amount of the extracted lithium ions is increased. In particular, the expansion of c in a cycle whose upper limit is set at 4.7 V is in $LiNi_{0.80}Co_{0.16}Al_{0.04}O_2$ about twice as large as that

(26) Cho, J. *Chem. Mater.* **2000**, *12*, 3089.
(27) Jeong, E.-D.; Won, M.-S.; Shim, Y.-B. *J. Power Sources* **1998**, *70*, 70.
(28) Delmas, C.; Menetrier, M.; Croguennec, L.; Saadoune, I.; Rougier, A.; Pouillerie, C.; Prado, G.; Grune, M.; Fournes, L. *Electrochim. Acta* **1999**, *45*, 243.
(29) Dahn, J. R.; von Sacken, U.; Michal, C. A. *Solid State Ionics* **1990**, *44*, 87.
(30) Li, W.; Reimers, J. N.; Dahn, J. R. *Solid State Ionics* **1993**, *67*, 123.
(31) Ohzuku, T.; Ueda, A. *J. Electrochem. Soc.* **1994**, *141*, 2972.

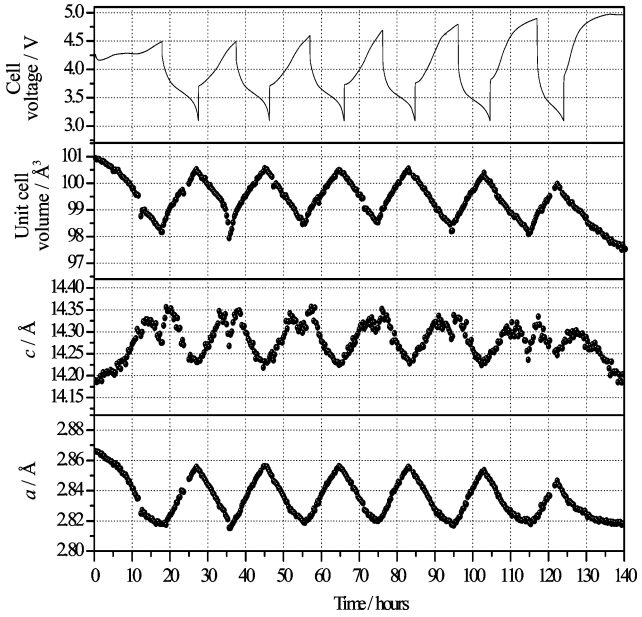

Figure 5. Time evolution of the cell voltage, lattice parameters (*a* and *c*), and unit cell volume of the $LiNi_{0.80}Co_{0.16}Mg_{0.04}O_2$ electrode. The latter were obtained by refining the diffraction patterns acquired upon the Li extraction−insertion process and reported in Figure 4.

in $LiNi_{0.80}Co_{0.16}Mg_{0.04}O_2$. This results in a very limited lattice expansion, as was clearly visible by looking at the unit cell volume curve, whose variation is <3% (∼5% in $LiNi_{0.80}Co_{0.16}Al_{0.04}O_2$ and ∼6% in $LiNi_{0.80}Co_{0.20}O_2$).[11,16]

Such a difference can be explained by considering that all of the Mg^{2+} ions are expected to migrate from the slab 3a to the interslab 3b sites upon cycling with high anodic voltage limits,[24,32] while Al^{3+} ions should not move from the slab 3a sites. The presence of cations other than Li^+ in the interslab sites ("pillaring" ions) results in an increased binding force between adjacent O−M−O slabs, which is responsible, in turn, for the reduced lattice expansion in the *z* direction (i.e., the *c* parameter variation is lower). In Mg-doped samples, the Mg^{2+} ions migrating in the interslab sites stabilize the structure as explained above. On the other hand, Al-doped samples present in the interslab sites (if any) only a small quantity of electrochemically active Ni^{2+} (Ni^{3+} ion migration from the slab to the interslab is expected to be harder than Mg^{2+} migration[32]) acting as pillaring ions, so that the *c* lattice parameter variation upon cycling is higher.

The reduced stretching of the *c* parameter upon cycling makes the intercalation−deintercalation process more reversible because it limits the structural strains that are one of the main causes for capacity loss upon prolonged cycling. It also allows the use of the doped oxide in a larger range of potential than that suitable for the undoped oxide, thus improving the capacity of the lithium ion cell. Furthermore, the ionic radius of Mg^{2+} (0.72 Å)[33] is comparable to that of Li^+ (0.76 Å),[33] and, Mg^{2+} being an electrochemically inactive ion, it does not change upon cycling. This fact consents a good Li^+ diffusion regardless of the oxidation state of the electrode. On the other hand, in Al-doped samples, Ni pillaring ions in the interslab sites can be oxidized at high voltage to Ni^{4+} ions, whose ionic radius (0.48 Å)[33] is much smaller. In this case, the Li^+ ion diffusivity is expected to be reduced at high voltage, spoiling the rate capability of a system with such an electrode.

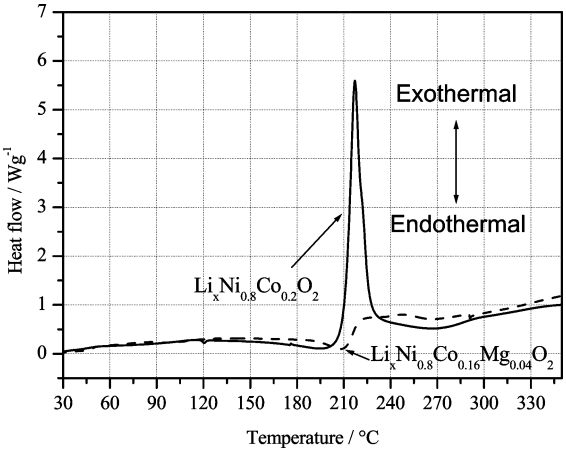

Figure 6. Differential scanning calorimetry (DSC) of commercial $LiNi_{0.8}Co_{0.2}O_2$ and of the $LiNi_{0.80}Co_{0.16}Mg_{0.04}O_2$ sample in the charged (delithiated) state. Heating rate = 5 °C min^{-1}.

In Figure 6, the comparison between the DSC curves obtained on delithiated commercial $Li_xNi_{0.8}Co_{0.2}O_2$ and on delithiated $Li_xNi_{0.8}Co_{0.16}Mg_{0.04}O_2$ powders is shown. The DSC profile of $Li_xNi_{0.8}Co_{0.2}O_2$ in its charged state shows a large exothermic peak at 215 °C, which confirms the instability of this material. This peak is associated with the reaction of molecular oxygen, released at high voltage by the cathodic material, with the electrolyte, which is understood as being one of the main causes of safety problems of Li-ion cells.[34−37] On the contrary, the DSC curve of the doped sample is quite flat over the entire temperature range, revealing only a small endothermic peak at 210 °C, probably associated with the electrolyte decomposition.[37,38] The thermal stability behavior can be attributed to the different cationic mixing between $LiNi_{0.8}Co_{0.2}O_2$ and $LiNi_{0.8}Co_{0.16}Mg_{0.04}O_2$, particularly in the charged state, in which, as discussed above, a migration of Mg^{2+} ions from the slab to interslab space is expected.[24,32] The presence of Mg^{2+} in the Li^+ site is thought to improve the interaction between Li^+ slabs and O−M−O layer, reducing the release of oxygen.

This is a further clear demonstration that the partial substitution of cobalt with Mg^{2+} stabilizes the oxide structure, inhibiting the thermal reaction otherwise occurring in the undoped $Li_xNi_{0.8}Co_{0.2}O_2$ parent compounds.

Conclusions

$LiNi_{0.8}Co_{0.16}Mg_{0.04}O_2$ was synthesized using a chemical route based on an optimized polymeric precursor

(32) Pouillerie, C.; Croguennec, L.; Delmas, C. *Solid State Ionics* **2000**, *132*, 15.
(33) Shannon, R. D.; Prewitt, C. T. *Acta Crystallogr., Sect. B* **1969**, *25*, 925.
(34) Cho, J.; Park, B. *J. Power Sources* **2001**, *92*, 35.
(35) Ohzuku, T.; Ueda, A.; Kouguchi, M. *J. Electrochem. Soc.* **1995**, *142*, 4033.
(36) Ohzuku, T.; Yanagawa; Kouguchi, M.; Ueda, A. *J. Power Sources* **1997**, *68*, 131.
(37) Arai, H.; Tsuda, M.; Saito, K.; Hayaci, M. *J. Electrochem. Soc.* **2002**, *149*, A401.
(38) Zhang, Z.; Fouchard, D.; Rea, J. R. *J. Power Sources* **1998**, *70*, 16.

decomposition process. The quality of the synthesis procedure was tested by TGA/DTA, SEM, ICP-AES, and XRD. In particular, Rietveld refinement on the XRD pattern showed little Ni ions disorder with Mg ions occupying 3a slab sites only. The in-situ EDXD structural characterization performed in this work has shown that doping with small amounts of Mg^{2+} dramatically reduces the expansion−contraction of the *c* lattice parameter with respect to the undoped ($LiNi_{0.8}Co_{0.2}O_2$) and to the Al-doped ($LiNi_{0.8}Co_{0.16}Al_{0.04}O_2$) mixed Ni−Co cathode during the lithium insertion−extraction process. Such reduction results in an overall unit cell volume variation <3% (∼5% in $LiNi_{0.80}Co_{0.16}Al_{0.04}O_2$ and ∼6% in $LiNi_{0.80}Co_{0.20}O_2$). This interesting result is likely due to the migration of Mg^{2+} ions from the slab (3a) to the interslab (3b) sites. A confirmation that such migration is the cause of the high thermal stability of $LiNi_{0.8}Co_{0.16}Mg_{0.04}O_2$ comes from DSC studies on the sample in its charged state, which does not exhibit the exothermal peak associated with the reaction involving oxygen release.

Due to these favorable properties, doped Ni−Co cathodes, for example, of the $LiNi_{0.80}Co_{0.16}Mg_{0.04}O_2$ type, may be regarded as an alternative to $LiCoO_2$, for the development of long-life, reliable, and safe lithium ion batteries.

CM040130X